

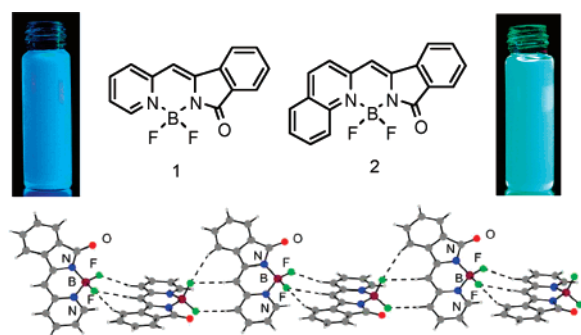
Novel Fluorescent Fluorine–Boron Complexes: Synthesis, Crystal Structure, Photoluminescence, and Electrochemistry Properties

Ying Zhou,[†] Yi Xiao,^{*,†} Dan Li,[†] Meiyun Fu,^{†,§} and Xuhong Qian^{*,‡}

State Key Laboratory of Fine Chemicals, Dalian University of Technology, Dalian 116012, China, Virtual Laboratory of Computational chemistry, CNIC Chinese Academy of Science, State Key Laboratory of Bioreactor Engineering and Shanghai Key Laboratory of Chemical Biology, East China University of Science and Technology, Shanghai 200237, China

xiaoyi@chem.dlut.edu.cn; xhqian@ecust.edu.cn

Received October 19, 2007



Two novel fluorine–boron cored fluorescent complexes were designed and synthesized. These two complexes displayed well-ordered molecular packing, intense fluorescence, and low LUMO levels. The results indicated their potential use as electron-transport materials in electroluminescent (EL) devices.

Organic fluorine–boron complexes, with the boron-dipyrromethene (BODIPY) as the best-known example, are a family with excellent fluorescent properties. Their intense fluorescence and tunable emission wavelength enable them to be widely applied as fluorescent sensors in the fields of analytical chemistry and biochemical chemistry.¹ The modification of the complexes' structures can not only adjust their optical properties² but also improve their electron-accepting and electron-transporting capabilities.^{3,4} Therefore, in recent years, the attention has

been paid to the design and synthesis of novel fluorine–boron complexes to explore their applications as photoelectric functional materials. Although a few F–B complexes have been reported as efficient charge-transport materials used in organic light-emitting diodes (OLED),³ or N-channel organic field-effect transistors (OFET),⁴ in general, the exploration of F–B complexes as charge-transport materials is still inadequate.

For electron-optical materials based on small molecules, well-ordered molecular packing is a favorable and critical factor in determining their electron-transporting properties.⁵ Regular packing is greatly affected by a number of intermolecular effects, such as hydrogen bonds and π – π stacking. So far, very few reports concerning intermolecular interactions involving F atom, e.g., C–H \cdots F–B, have been found in the crystal studies of F–B complexes,⁶ especially in the electron-optical materials.

Bearing these facts in mind, we designed and synthesized a series of novel F–B cored fluorescent compounds as potential charge-transport materials, with the C–H \cdots F–B working as a major influencing factor on their regular crystal packing. Molecular structures of compounds **1** and **2** are illustrated in Scheme 1. In these molecules with relatively large conjugation systems, the molecular frames were of good planarity, and no side chain had been introduced, which favored the compact molecular packing. Moreover, for their application as effective and competitive electron-transport materials, the groups with low electron density, such as pyridine, quinoline, and imide, had been chosen as the compositions of the ligands to have deep LUMO levels with strong electron-accepting ability.

The synthetic routes of compounds **1** and **2** are depicted in Scheme 2. Starting from compound **3**, two different ways were adopted in the preparation of **5**, the immediate precursor of **1**. In route A, upon the heating of a 1:2:2 mixture of **4**, 2-pyridylaldehyde and K_2CO_3 at 100 °C for 10 h in toluene, **5** was obtained in a 68% yield. Meanwhile, **6** was synthesized with yield of 60% by the similar condensation of **4** and quinoline-2-carbaldehyde. On the other hand, in route B, the condensation reaction of **3** and 2-methylpyridine using fresh melted zinc chloride without solvent was carried out to give **5** in 74% yield. Compared with route A, route B was more effective and less complicated. Thus, we established the route B as having the optimum reaction conditions for the preparation of **5**.

It was found that *N*-ethyl-diisopropylamine could efficiently promote the coordination between ligand **5** or **6** and BF_3 , even at room temperature, while this reaction did not occur or

(2) (a) Liu, D.; Mudadu, M.; Thummel, R.; Tao, Y.; Wang, S. *Adv. Funct. Mater.* **2005**, *15*, 143–154. (b) Li, Y.; Liu, Y.; Guo, J.; Wang, Y. *Chem. Commun.* **2000**, 1551–1552. (c) Dost, Z.; Atilgan, S.; Akkaya, E. U. *Tetrahedron* **2006**, *62*, 8484–8488.

(3) Domercq, B.; Grasso, C.; Maldonado, J.-L.; Halik, M.; Barlow, S.; Marder, S. R.; Kippelen, B. *J. Phys. Chem. B* **2004**, *108*, 8647–8651.

(4) Sun, Y.; Rohde, D.; Liu, Y.; Wan, L.; Wang, Y.; Wu, W.; Di, C.; Yu, G.; Zhu, D. *J. Mater. Chem.* **2006**, *16*, 4499–4503.

(5) (a) Cornil, J.; Beljonne, D.; Calbert, J. P.; Bredas, J. L. *Adv. Mater.* **2001**, *13*, 1053–1067. (b) Schön, J. H.; Berg, S.; Kloc, C.; Batlogg, B. *Science* **2000**, *287*, 1022–1023.

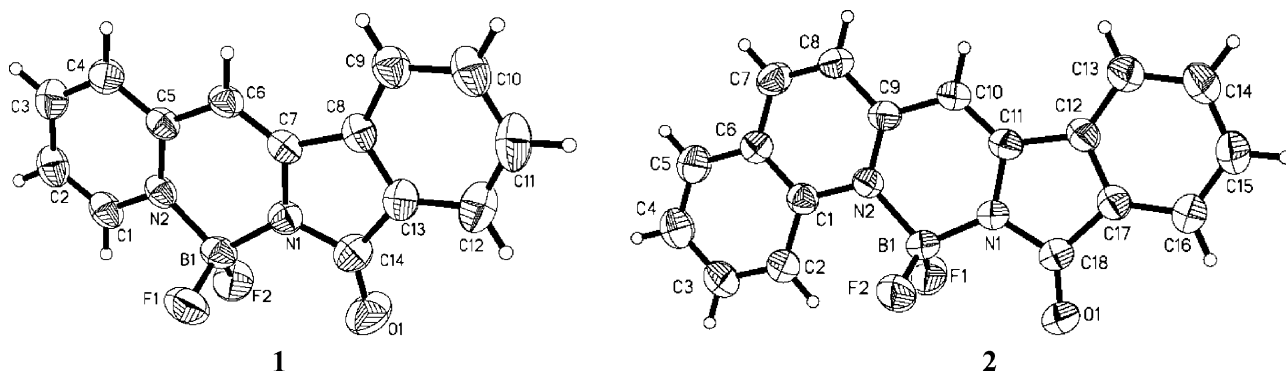
(6) (a) Camerel, F.; Bonardi, L.; Ulrich, G.; Charbonniere, L.; Donnio, B.; Bourgoigne, C.; Guillon, D.; Retailleau, P.; Ziessel, R. *Chem. Mater.* **2006**, *18*, 5009–5021. (b) Duniz, J. D. *ChemBioChem* **2004**, *5*, 614–621. (c) Clarke, C. M.; Das, M. K.; Henecker, E.; Mariategui, J. F.; Niedunzu, K.; Niedenzu, P. M.; Noth, H.; Warner, K. R. *Inorg. Chem.* **1987**, *26*, 2310–2317.

[†] State Key Laboratory of Fine Chemicals, Dalian University of Technology.

[§] Virtual Laboratory of Computational chemistry, CNIC Chinese Academy of Science.

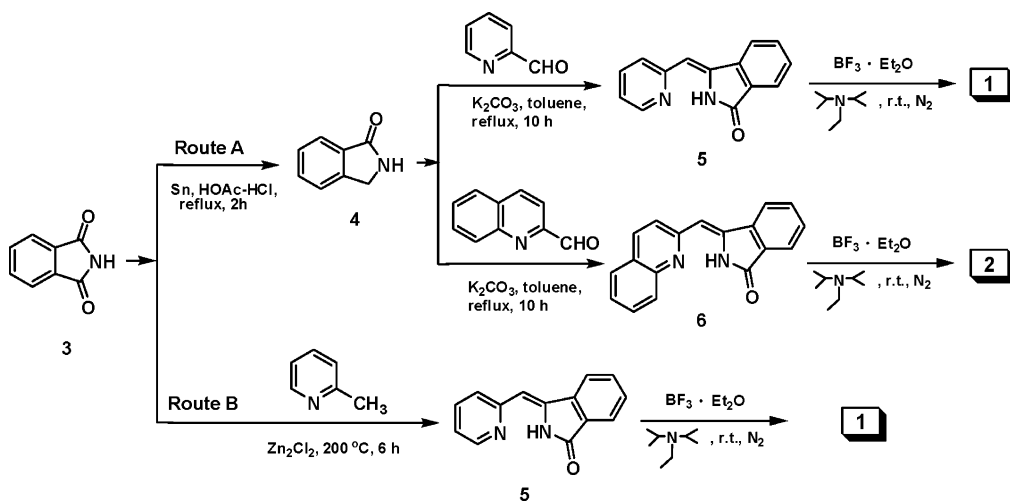
[‡] East China University of Science and Technology.

(1) (a) Coskun, A.; Akkaya, E. U. *J. Am. Chem. Soc.* **2005**, *127*, 10464–10465. (b) Bricks, J. L.; Kovalchuk, A.; Trieflinger, C.; Nofz, M.; Buschel, M.; Tolmachev, A. I.; Daub, J.; Rurack, K. *J. Am. Chem. Soc.* **2005**, *127*, 13522–13529. (c) Yamada, K.; Nomura, Y.; Citterio, D.; Iwasawa, N.; Suzuki, K. *J. Am. Chem. Soc.* **2005**, *127*, 6956–6957. (d) Coskun, A.; Akkaya, E. U. *J. Am. Chem. Soc.* **2006**, *128*, 14474–14475. (e) Camerel, F.; Bonardi, L.; Schmutz, M.; Ziessel, R. *J. Am. Chem. Soc.* **2006**, *128*, 4548–4549. (f) Coskun, A.; Yilmaz, M. D.; Akkaya, E. U. *Org. Lett.* **2007**, *9*, 607–609.

SCHEME 1. Perspective Views of Crystal 1 and 2, Including Atom Numbering Scheme^a

^a Thermal ellipsoids are at 50% probability level for C, O, and N atoms.

SCHEME 2. Synthetic Routes of Compounds 1 and 2



occurred with very low yield in the presence of other bases. Stirring of the mixture of precursors **5** or **6**, *N*-ethyl-diisopropylamine and BF_3 , at room temperature under N_2 , directly gave compounds **1** and **2** in yields of 50% and 55%, respectively.

These findings were significant, since the synthetic route **B** in the present work could provide a facile and efficient substitute for the previous approaches to BODIPY analogues.

Crystal Structure of 1. The F–B–F group in **1** acted as a bifurcated acceptor with an angle of 109.88° , and both of the F atoms formed C–H \cdots F–B contacts with the neighboring donor molecule (Supporting Information). The mean deviation from the whole molecular plane except for the B–F group was 0.0723 Å, which showed the good planarity of the main molecular plane. Adjacent molecules were linked by C–H \cdots F–B interactions to form a “zigzag chain” as shown in Figure 1. It indicated that an offset π – π stacking was formed between the paralleled chains in crystal **1**⁷ (Supporting Information).

Most of the current crystal studies on the C–F group,⁸ the so-called “organic fluorine”, showed that the fluorine atom was unable to compete favorably with O and N atom acceptors.⁹

However, the occurrence of C–H \cdots F–B interactions and the absence of a C–H \cdots O interaction in **1** suggested a clear influencing factor of B–F on the packing modes. Therefore, we viewed that the F atom in a BF complex was a stronger hydrogen bond acceptor than “organic fluorine” and it could compete with other strong acceptors such as the O atom.

Crystal Structure of 2. In **2**, one of the F atoms (F1) acted as a hydrogen acceptor, but the other F atom (F2) was not involved in the hydrogen bonds. Each molecule of **2** was connected with its neighbors via two C–H \cdots F–B H bonds and two C–H \cdots O H bonds (Supporting Information). The mean deviation from the whole molecular plane except for the F–B–F group was 0.0638 Å. The planar molecules aligned parallel to each other to form “columns” along the *a*-axis. (Figure 2) For **2**, molecules parallel to each other along one-dimensional molecular columns could act as channels for electron transport, producing high carrier mobility.

Obviously, the size of the quinoline group was larger than that of pyridine. When the quinoline group was introduced in juxtaposition to the B–F center in **2**, this geometry change enhanced the steric hindrance around the central B–F bond and led to a different H bond binding mode from that in **1**. Meanwhile, the large difference in the steric requirement resulted in the different performances of the O atoms in these two compounds.

Photoluminescence and Electrochemistry Studies. BODIPY derivatives are well-known for their narrow absorption

(7) Planas, J. G.; Masalles, C.; Sillanpaal, R.; Kiveias, R.; Teixidor, F.; Vinas, C. *CrystEngComm* **2006**, *8*, 75–83.

(8) (a) Bayon, R.; Coco, S.; Espinet, P. *Chem. Eur. J.* **2005**, *11*, 1079–1085. (b) Dunita, J. D.; Schweizer, W. B. *Chem. Eur. J.* **2006**, *12*, 6804–6815. (c) Kasai, K.; Fujita, M. *Chem. Eur. J.* **2007**, *13*, 3089–3105.

(9) (a) Schwarzer, A.; Seichter, W.; Weber, E.; Stoeckli-Evans, H.; Losada, M.; Hulliger, J. *CrystEngComm* **2004**, *6*, 567–572. (b) Choudhury, A. R.; Nagarajan, K.; Guru Row, T. N. *Cryst. Eng.* **2003**, *6*, 145–152.

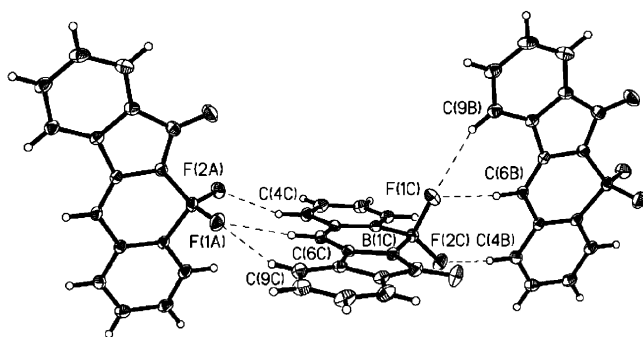


FIGURE 1. Views of hydrogen bonding via the C–H...F–B contacts in crystal 1.

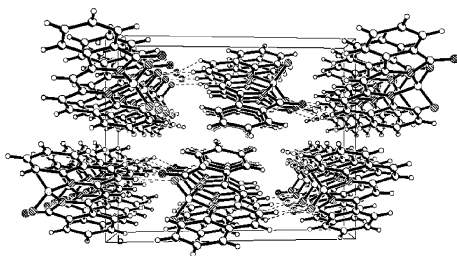


FIGURE 2. Packing diagrams along the *a*-axis, showing the π – π contacts and network in crystal 2.

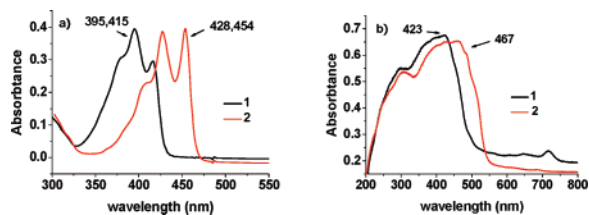


FIGURE 3. Absorption spectra of compounds 1 and 2 in dichloromethane (a) and in solid state (b).

and emission bands, little Stokes shifts, and high fluorescence quantum yields in solution.¹⁰ Contrastively, broad absorption bands, large Stokes shifts, and strong fluorescence both in solution and in solid state were found for our two BF complexes.

The absorption and emission maximums of **2** were considerably red-shifted compared to those of **1**, due to the enlarged conjugation system in **2**.

In dichloromethane, **1** had a major absorption peak at 395 nm, and **2** had two absorption peaks at 428 and 454 nm. (Figure 3) In ethanol, tiny blue shifts were observed. In solid state, their absorption bands got much broader than in solution.

Compounds **1** and **2** exhibited intensive fluorescence in solution. For example, quantum yields in dichloromethane were 0.47 for **1** and 0.49 for **2**. In dichloromethane, the emission maximum of **1** was at 454 nm with a 58 nm Stokes shift, and emission peaks of **2** were at 464 and 492 nm, with a 38 nm Stokes shift. The Stokes shifts of these compounds were quite larger than those of many BODIPYs.

Unlike BODIPYs, **1** and **2** also showed remarkable fluorescence in solid state, as displayed in Figure 4. We assumed that the large Stokes shifts partly offset the self-quench effect in

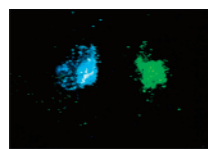


FIGURE 4. Photo of solid fluorescence of **1** (left) and **2** (right), which was taken under a handheld UV (365 nm) lamp.

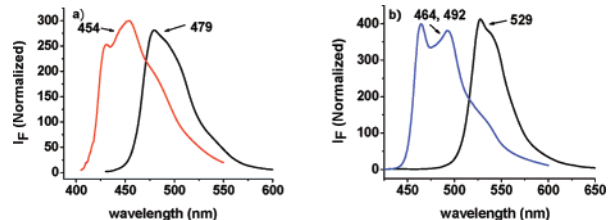


FIGURE 5. Fluorescence emission spectra of **1** (a) and **2** (b) in dichloromethane and in solid state.

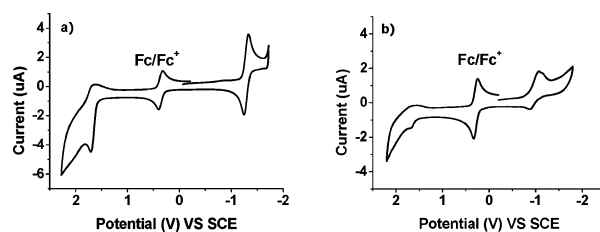


FIGURE 6. Cyclic voltammograms of **1** (a) and **2** (b) measured in CH₃CN solution, containing 0.1 M TBAPF₆ at 20 °C. Ferrocene (Fc) was used as internal reference, and potentials were calculated as relative to the SCE assuming that $E_{1/2}$ (Fc/Fc⁺) +0.38 V (ΔE_p 70 mV) vs SCE.

solid state. The emission maximum of **1** red-shifted to 479 nm, and the emission bands of **2** red-shifted to 529 nm, which could be attributed to the π – π stacking induced by the more compact molecular packing in the solid state (Figure 5).

The electronic states (HOMO/LUMO levels) of **1** and **2** were investigated by cyclic voltammetry (CV). As shown in Figure 6, **1** and **2** both exhibited reversible reduction waves. The estimated electron affinity (EA, LUMO level) values were –3.22 eV for **1** and –3.45 eV for **2**. For comparison, the electronic states of BODIPY were tested (Supporting Information). It showed the LUMO values of the two compounds were considerably lower than those of BODIPY (–3.05 eV) and the most popular electron-transport material Alq₃ (–3.0 eV).¹¹ The ionization potential (IP, HOMO level) of **1** and **2** were –6.07 and –6.05 eV, respectively. These HOMO values were also lower than those of BODIPY (–5.45 eV) and Alq₃ (–5.7 eV).¹¹

Through these comparisons, it was clear that **1** and **2** had better electron-accepting features, which enhanced their potential charge-transport properties of interest for practical applications.

For better understanding of spectra and electron properties displayed by **1** and **2**, we carried out molecular orbital calculations for these compounds on the density functional theory (DFT) level using a B3LYP/6-31G basis set, employing the Gaussian 03 suit of programs.¹² Geometric parameters from X-ray diffraction analysis were used for the calculation. Figure 7 shows HOMO and LUMO levels of **1** and **2**.

(10) (a) Yogo, T.; Urano, Y.; Ishitsuka, Y.; Maniwa, F.; Nagano, T. *J. Am. Chem. Soc.* **2005**, *127*, 12162–12163. (b) Oleynik, P.; Ishihara, Y.; Cosa, G. *J. Am. Chem. Soc.* **2007**, *129*, 1842–1843.

(11) Burrows, P. E.; Shen, Z.; Bulovic, V.; McCarty, D. M.; Forrest, S. R.; Cronin, J. A.; Thompson, M. E. *J. Appl. Phys.* **1996**, *79*, 7991–8006.

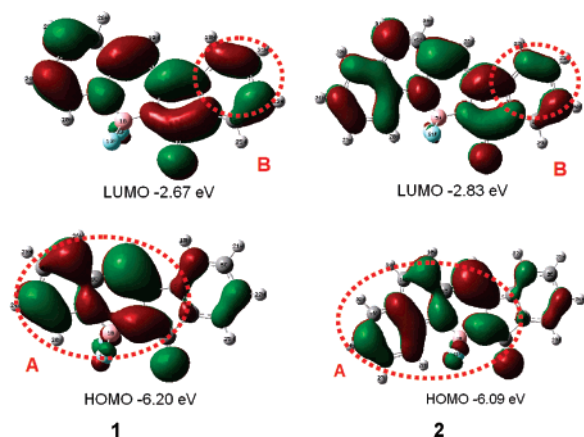


FIGURE 7. Diagrams showing the HOMO and LUMO levels of **1** and **2**.

TABLE 1. Values of the Electronic States (HOMO/LUMO Levels) and Energy Gap (eV)

cmpd	LUMO		HOMO		E_g		
	V_{cv}	V_{ca}	V_{cv}	V_{ca}	V_{cv}	V_{ca}	V_{UV}
1	-3.22	-2.67	-6.07	-6.20	2.85	3.53	2.54
2	-3.45	-2.83	-6.05	-6.09	2.60	3.26	2.32

^a V_{cv} : the value from cyclic voltammetry; V_{ca} : the value from MO calculation; V_{UV} : the value estimated by using the UV-vis absorption edge.

The diagrams of the HOMO and LUMO levels of TM-BODIPY were studied for comparison (Supporting Information). It showed that the HOMO and LUMO levels of TM-BODIPY were delocalized in the whole atomic part, with small differences in the dipole moments.¹³ In the present work, the LUMO distribution of both compounds was donated by all atomic orbitals in the aromatic rings, while contributions to the HOMO distribution were mainly from part A. Therefore, intramolecular charge transfer (ICT) from part A to part B was suggested in **1** and **2**, which could partly explain their broad bands in absorption¹⁴ and large Stokes shifts.¹⁵

The calculated HOMO–LUMO band gap of **1** was larger than that of **2**, which was consistent with the trend of the spectra. (Table 1) The increased conjugation system in **2** reduced the LUMO energy effectively but the HOMO energy weakly, hence red-shifting both absorption and emission spectra.

(12) Frisch, M. J.; Trucks, G. W.; Schlegel, H. B.; Scuseria, G. E.; Robb, M. A.; Cheeseman, J. R.; Montgomery, J. A., Jr.; Vreven, T.; Kudin, K. N.; Burant, J. C.; Millam, J. M.; Iyengar, S. S.; Tomasi, J.; Barone, V.; Mennucci, B.; Cossi, M.; Scalmani, G.; Rega, N.; Petersson, G. A.; Nakatsuji, H.; Hada, M.; Ehara, M.; Toyota, K.; Fukuda, R.; Hasegawa, J.; Ishida, M.; Nakajima, T.; Honda, Y.; Kitao, O.; Nakai, H.; Klene, M.; Li, X.; Knox, J. E.; Hratchian, H. P.; Cross, J. B.; Adamo, C.; Jaramillo, J.; Gomperts, R.; Stratmann, R. E.; Yazyev, O.; Austin, A. J.; Cammi, R.; Pomelli, C.; Ochterski, J. W.; Ayala, P. Y.; Morokuma, K.; Voth, G. A.; Salvador, P.; Dannenberg, J. J.; Zakrzewski, V. G.; Dapprich, S.; Daniels, A. D.; Strain, M. C.; Farkas, O.; Malick, D. K.; Rabuck, A. D.; Raghavachari, K.; Foresman, J. B.; Ortiz, J. V.; Cui, Q.; Baboul, A. G.; Clifford, S.; Cioslowski, J.; Stefanov, B. B.; Liu, G.; Liashenko, A.; Piskorz, P.; Komaromi, I. R.; Martin, L.; Fox, D. J.; Keith, T.; Al-Laham, M. A.; Peng, C. Y.; Nanayakkara, A.; Challacombe, M.; Gill, P. M. W.; Johnson, B.; Chen, W.; Wong, M. W.; Gonzalez, C.; Pople, J. A. *Gaussian 03*, Revision B.05; Gaussian, Inc.: Pittsburgh, PA, 2003.

(13) Bergstrom, F.; Mikhalyov, I.; Hagglof, P.; Wortmann, R.; Ny, T.; Johansson, L. *J. Am. Chem. Soc.* **2002**, *124*, 196–204.

(14) Cui, Y.; Liu, Q.; Bai, D.; Jia, W.; Tao, Y.; Wang, S. *Inorg. Chem.* **2005**, *44*, 601–609.

(15) Peng, X.; Song, F.; Lu, E.; Wang, Y.; Zhou, W.; Fan, J.; Gao, Y. *J. Am. Chem. Soc.* **2005**, *127*, 4170–4171.

In summary, two novel F–B cored fluorescent complexes were designed and efficiently synthesized. Their crystal structures and photophysical and electrochemical properties were investigated. The well-ordered molecular packing, strong luminescence, and low LUMO levels indicated their potential as electron-transport materials in electroluminescent (EL) devices. Efforts for further electron-optical applications are underway.

Experimental Section

Compound 5: Route A. A solution of compound **4** (0.40 g, 3 mmol), 2-pyridylaldehyde (0.64 g, 6 mmol), and K_2CO_3 (0.80 g, 6 mmol) in 20 mL of toluene was heated to 100 °C for 12 h. Toluene was removed in vacuum, and the resulting mixture was extracted with dichloromethane. The extract was purified by silica gel column chromatography using ethyl acetate as eluent to afford compound **5**. Yield: 0.44 g (68%). The products were used without further purifications.

Route B. In a sealed kettle 1.00 g of **3** (6.8 mmol), 3 mL of 2-methylpyridine (34 mmol), and 0.20 g of fresh melted zinc chloride were mixed together and heated at 170 °C for 6 h. The resulting brown mixture was extracted with water/dichloromethane. The extract was purified by silica gel column chromatography using ethyl acetate as eluent to afford compound **5**. Yield: 1.11 g (74%).

Compound 1. To the solution of 0.17 g of **5** (0.75 mmol) in 10 mL of CH_2Cl_2 were added 0.4 mL of *N*-ethyl-diisopropylamine and 1 mL of $BF_3 \cdot Et_2O$. The mixture was stirred under nitrogen for 3 h at room temperature. The residues were purified by silica gel column chromatography using dichloromethane as eluent to afford compound **1**. Yield: 0.1 g (50%), mp: 247–249 °C. 1H NMR (500 MHz, DMSO) δ 6.96 (s, H), 7.68–7.72 (m, 2H), 7.77–7.81 (m, H), 7.84 (s, H), 7.86 (s, H), 8.06–8.08 (d, H), 8.31–8.34 (m, H), 8.75–8.77 (d, H); ^{13}C NMR (100 MHz, DMSO) δ 94.7, 122.1, 123.1, 123.6, 125.4, 130.3, 131.9, 133.3, 136.0, 142.5, 143.7, 144.7, 149.4, 170.5; TOF MS EI^+ : calcd for $C_{14}H_9BF_2N_2O$ 270.0776, found 270.0781.

Compound 2. Starting from compound **3** (0.40 g, 3 mmol), 2-quinoline carbaldehyde (0.94 mL, 6 mmol), and K_2CO_3 (0.80 g, 6 mmol) in 20 mL of toluene, compound **6** was synthesized and purified by a procedure similar to that of route A for compound **5** described above. Yield: 0.48 g (60%).

To the solution of 0.217 g of compound **6** (0.8 mmol) in 10 mL of CH_2Cl_2 were added 0.5 mL of *N*-ethyl-diisopropylamine and 1 mL of $BF_3 \cdot Et_2O$. The mixture was stirred under nitrogen for 3 h at room temperature. The residues were purified in a way similar to that for purifying compound **1**. Yield: 0.141 g (55%), mp: 278–280 °C. 1H NMR (500 MHz, DMSO) δ 7.07 (s, H), 7.75–7.78 (m, 2H), 7.82–7.85 (m, 2H), 7.89–7.90 (d, H), 7.98–8.02 (m, H), 8.13–8.17 (m, 2H), 8.71–8.73 (d, H), 8.77–8.78 (d, H); ^{13}C NMR (400 MHz, DMSO) δ 95.6, 122.7, 123.4, 123.9, 127.5, 127.6, 129.8, 130.4, 132.5, 133.0, 133.6, 135.4, 143.7, 152.9; TOF MS EI^+ : calcd for $C_{18}H_{11}BF_2N_2O$ 320.0932, found 320.0936.

Acknowledgment. This work was supported by NSF of China (No. 20406004, 20572012, 20536010). We also thank Dr. Cheng He for the suggestions on the crystallographic analyses.

Supporting Information Available: General experimental methods, compound characterization data, crystallographic information files (CIF), crystallographic analyses based on X-ray determination and related H-bond data for **1** and **2**. This material is available free of charge via the Internet at <http://pubs.acs.org>.

JO702265X